Journal of Integrative Neuroscience

J. Integr. Neurosci. **2026**; 25(7): 50442
https://doi.org/10.31083/JIN50442

Short Communication

Sevoflurane and $A\beta_{1-42}$ Oligomers Synergistically Induce Morphological Changes of Astrocytes in the Hippocampus of Male Mice

Qinfang Shi[1,2,†], Arpit Kumar Pradhan[3,†], Siwei Dong[1,2], Gerhard Rammes[4,5,*], Xingxing Wang[6,*]

[1]Department of Anesthesiology, Union Hospital, Tongji Medical College, Huazhong University of Science and Technology, 430022 Wuhan, Hubei, China
[2]Key Laboratory of Anesthesiology and Resuscitation (Huazhong University of Science and Technology), Ministry of Education, 430022 Wuhan, Hubei, China
[3]Department of Psychology, University of Michigan, Ann Arbor, MI 48109, USA
[4]Department of Anesthesiology and Intensive Care Medicine, School of Medicine and Health, Klinikum Rechts der Isar, Technical University of Munich, 81675 Munich, Germany
[5]Graduate School of Systemic Neuroscience, Ludwig Maximilian University of Munich, 82152 Munich, Germany
[6]School of Integrative Medicine, Shanghai University of Traditional Chinese Medicine, 201203 Shanghai, China
*Correspondence: g.rammes@tum.de (Gerhard Rammes); xingxingwangchn@163.com (Xingxing Wang)
[†]These authors contributed equally.

Academic Editor: Zhi Dong Zhou
Submitted: 27 January 2026 Revised: 22 May 2026 Accepted: 11 June 2026 Published: 29 July 2026

Abstract

Background: Reactive gliosis serves as a characteristic feature of the pathophysiology of Alzheimer's disease (AD). Nevertheless, the influence of anesthetics on the morphological dynamics of astrocytes remains ambiguous. **Methods:** Employing *ex vivo* hippocampal slices, in this study, we explored the impacts of sevoflurane and Amyloid-β peptide 1-42 ($A\beta_{1-42}$) oligomers on astrocytic morphology. The primary outcomes encompassed the fluorescence intensity of glial fibrillary acidic protein (GFAP), the levels of a 38-kDa GFAP breakdown product (a marker of astroglial injury), and quantitative morphometric analyses (cell volume, surface area, branch complexity, and Sholl intersections). **Results:** Co-exposure to sevoflurane and $A\beta_{1-42}$ led to an elevation of the 38-kDa GFAP breakdown product and a significant reduction in the mean fluorescence intensity of GFAP. Moreover, it resulted in a decrease in astrocytic volume, surface area, branch complexity, and Sholl intersections. These synergistic alterations were not observed when either treatment was administered alone. **Conclusions:** These findings imply that sevoflurane aggravates $A\beta_{1-42}$-induced astrocytic dysfunction, which has implications for perioperative management in patients with AD or those at risk of developing AD.

Keywords: Alzheimer's disease; sevoflurane; astroglial injury; glial fibrillary acidic protein

1. Introduction

Alzheimer's disease (AD) is a progressive neurodegenerative disorder that is characterized by memory impairment and a gradual decline in cognitive function. It is frequently associated with an elevated level of amyloid-beta (Aβ) in the brain. The pathophysiology of AD is mainly ascribed to the extracellular deposition of Aβ, the formation of hyperphosphorylated tau aggregates, and reactive gliosis [1]. Specifically, it has been demonstrated that $A\beta_{1-42}$ oligomers can impede Cornu Ammonis 1 (CA1) long-term potentiation, a cellular mechanism that exhibits a strong correlation with memory and learning [2].

The influence of general anesthetics on AD pathology presents conflicting findings. Some studies report a worsening effect, while others propose potential neuroprotective effects, which may reflect concentration-dependent and anesthetic-specific impacts [3,4]. Sevoflurane, a frequently utilized inhalational anesthetic, enhances caspase activation, β-secretase level, and the formation of Aβ aggregates in the brains of rodents with AD [3]. Our prior research demonstrated the concentration-dependent influence of sevoflurane on dendritic spine density and synaptic pruning by astrocytes in the presence of various Aβ species [5]. Reactive astrocytes are significantly involved in the pathology of AD. Their highly dynamic morphological characteristics are inherently associated with their functions, as evidenced in AD, where the loss of astrocytic branching may lead to impaired clearance of Aβ [6]. However, the combined influence of sevoflurane and Aβ on astrocyte morphology remains uninvestigated. Comprehending these effects would offer fresh perspectives on how anesthetics affect AD-associated astrocytic functions and may uncover novel pathways of disease advancement.

Glial fibrillary acidic protein (GFAP), an intermediate filament protein specific to astrocytes, preserves the mechanical integrity of astrocytes [7]. Crucially, GFAP mediates the development of reactive astrogliosis, which is the conserved response of the central nervous system to injury. Dysregulation of GFAP expression indicates altered astrocyte activity, which is correlated with neural dam-

age. During injury or neurodegeneration (e.g., AD), calpain cleaves GFAP into GFAP-derived breakdown products (GFAP BDPs), and this has been regarded as a potential marker of astroglial injury [8,9,10]. This study explored how sevoflurane and $A\beta_{1\text{-}42}$ affect astrocyte morphology and AD pathology.

2. Materials and Methods

2.1 Animals

A total of 32 adult male C57BL/6 mice, aged between 8–12 weeks, were obtained from the Animal Center of Shanghai University of Traditional Chinese Medicine. These mice were housed under controlled environmental conditions, including a 12-hour(h) light/dark cycle, a temperature of 22 ± 2 °C, and a relative humidity of 60%. The animals were provided with ad libitum access to food and water. The protocols were designed with a focus on minimizing the use of animals and reducing their discomfort.

2.2 Preparation of Acute Hippocampal Brain Slices

Mice were placed in an anesthesia chamber and anesthetized using 5% isoflurane (#400806.00.00, CP-Pharma, Burgdorf, Germany) for approximately 1 minute until the loss of the righting reflex, after which they were decapitated, and their brains were extracted into ice-cold cutting solution (self made, containing: 125 mM NaCl, 2.5 mM KCl, 25 mM $NaHCO_3$, 0.25 mM $CaCl_2$, 6 mM $MgCl_2$, 25 mM D-glucose, and 1.25 mM NaH_2PO_4). Sagittal hippocampal slices with a thickness of 400 µm were sectioned using a vibratome (VT1000 S, Leica Microsystems, Deer Park, IL, USA) and incubated in carbogenated artificial cerebrospinal fluid (aCSF, self made, containing: 125 mM NaCl, 2.5 mM KCl, 25 mM $NaHCO_3$, 2 mM $CaCl_2$, 1 mM $MgCl_2$, 25 mM D-glucose, and 1.25 mM NaH_2PO_4) at 35 °C for 30 minutes, followed by incubation at room temperature (21–24 °C) for 60 minutes. Subsequently, the slices were exposed for 3 h to the following conditions, respectively: carbogen (#10021938, Linde, Germany) alone, carbogen for 1.5 h followed by 1.2 minimum alveolar concentration (MAC) sevoflurane (CA2L9117, Baxter, Deerfield, IL, USA) for 1.5 h, 50 nM $A\beta_{1\text{-}42}$ (H-1368, Bachem, Bubendorf, Switzerland), or 50 nM $A\beta_{1\text{-}42}$ for 1.5 h and 1.2 MAC sevoflurane for 1.5 h.

2.3 $A\beta_{1\text{-}42}$ Preparation

$A\beta_{1\text{-}42}$ was suspended in 100% hexafluoroisopropanol (HFIP, #105228, Sigma-Aldrich, Darmstadt, Germany) at a concentration of approximately 1 mg per 400 µL of HFIP. The suspension was shaken at 37 °C for 1.5 h, aliquoted into tubes at a quantity of 100 µg per tube, and subsequently, the HFIP was evaporated. The dried aliquots were stored at –80 °C. For experimental purposes, the aliquots were dissolved in dimethyl sulfoxide (DMSO, 67-68-5, Sigma-Aldrich) and then diluted in aCSF solution to a working concentration of 50 nM.

2.4 Western Blot

The hippocampi were dissected, homogenized in a lysis buffer (Protease Inhibitor Cocktail tablets (11836170001, Roche, Basel, Switzerland); Pepstatin (#7626, Sigma-Aldrich); RIPA buffer (R0278, Sigma-Aldrich)), subjected to centrifugation, and the protein concentration in the supernatant was determined. The proteins were separated via sodium dodecyl sulfate-polyacrylamide gel electrophoresis (SDS-PAGE), transferred, blocked, and incubated overnight at 4 °C with primary antibodies (mouse anti-GFAP, 1:1000, #3450, Cell Signaling Technology, Danvers, MA, USA; rabbit anti-glyceraldehyde-3-phosphate dehydrogenase (GAPDH; 1:5000, #5174, Cell Signaling Technology)). Horseradish peroxidase (HRP)-conjugated secondary antibodies (1:10,000, #7074, Cell Signaling Technology) were then applied. The bands were detected using enhanced chemiluminescence (ECL, #34580, Thermo Fisher Scientific, Waltham, MA, USA), quantified, and the GFAP was normalized to GAPDH/total protein [5].

2.5 Quantification of the Mean Fluorescence Intensity (MFI) of GFAP

Confocal images of CA1 stratum radiatum GFAP were obtained using a Leica SP8 confocal microscope (Leica SP8, Wetzlar, Germany) with a 20× objective lens (NA = 0.75), employing parameters standardized for control samples. Z-stacks with a step size of 1 µm and approximately 20 slices were captured in a single session. Subsequently, the Z-stacks were transformed into 3D projections using ImageJ software (#1.8.0.345, National Institutes of Health, Bethesda, MD, USA). Regions of interest free from vessels and artifacts were manually selected using the Freehand Selection tool. The MFI was measured by setting the measurement parameters to the Mean Gray Value under the Analyze menu.

2.6 Astrocyte Morphology and the Sholl Analysis

Astrocytes were imaged using the Leica SP8 [11]. In each murine subject, we conducted quantification of 8–12 astrocytes (specifically sourced from the stratum radiatum of the CA1 region). With a sample size of 6–8 mice per group (n = 6–8), a total of 50–70 astrocytes per group were subjected to analysis. Morphological reconstruction (surfaces, filaments) was carried out in accordance with a paper by utilizing Imaris software 9.9.0 (Bitplane AG, Zurich, Switzerland) [12]. In brief, a novel surface was created using the original astrocyte image, and this surface was masked as a distinct channel. Filament reconstruction was carried out using the established surface, with Imaris supplying the starting/seed points. The starting point was adjusted to be precisely positioned at the center of the astrocyte soma, and the seed points were aligned with the astrocyte branching (bifurcation) points. The reconstruction was finalized, and the filament data were exported for analysis.

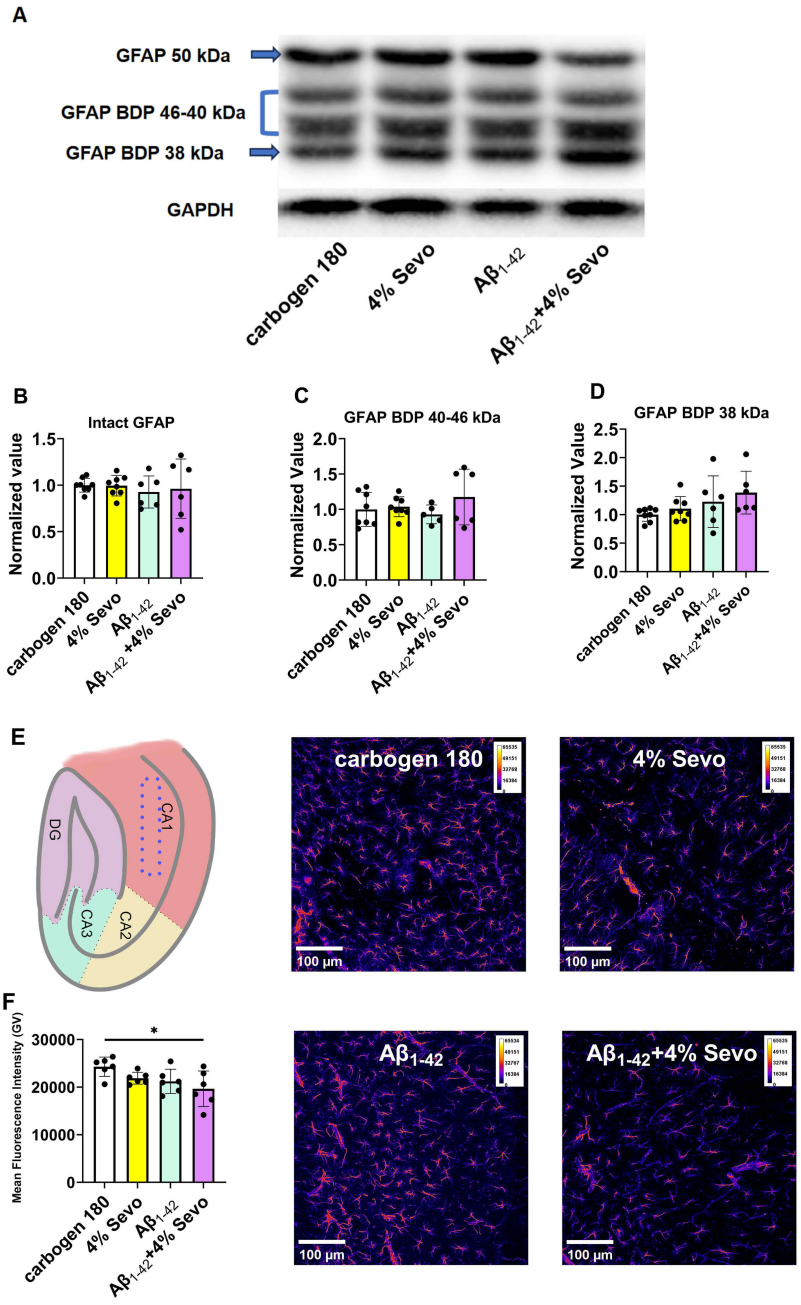

Fig. 1. Co-exposure to sevoflurane and Aβ$_{1-42}$ oligomers tends to increase 38-kDa glial fibrillary acidic protein (GFAP) breakdown product (BDP) levels and reduce astrocyte GFAP mean fluorescence intensity (MFI). (A) Representative western blot bands showing glyceraldehyde-3-phosphate dehydrogenase (GAPDH), intact GFAP, and its BDPs. (B–D) Quantification of intact GFAP (B), the 40–46 kDa BDPs (C), and the 38-kDa BDP (D) across experimental groups. (E) Schematic representation of hippocampal subregions; the stratum radiatum within the CA1 subfield is demarcated by a blue dashed box (left). Representative images of the hippocampal imaging area and astrocytes in different treatment groups (right). Scale bar, 100 μm. (F) Comparison of GFAP MFI among groups. Sevoflurane (Sevo). Data are presented as mean ± standard error of the mean (SEM), with individual animals represented by dots (carbogen 180 : n = 8 (B–D), n = 6 (F); 4% Sevo: n = 8 (B–D), n = 6 (F); Aβ$_{1-42}$: n = 6 (B,D,F), n = 5 (C); Aβ$_{1-42}$+4% Sevo: n = 6 (B,C,D,F)). Statistical significance was determined by one-way analysis of variance (ANOVA) with Bonferroni's post hoc test for multiple comparisons. * $p < 0.05$. Data point (black dots) represents the number of animals. Aβ, amyloid-beta; CA, Cornu Ammonis; DG, dentate gyrus; Sevo, sevoflurane.

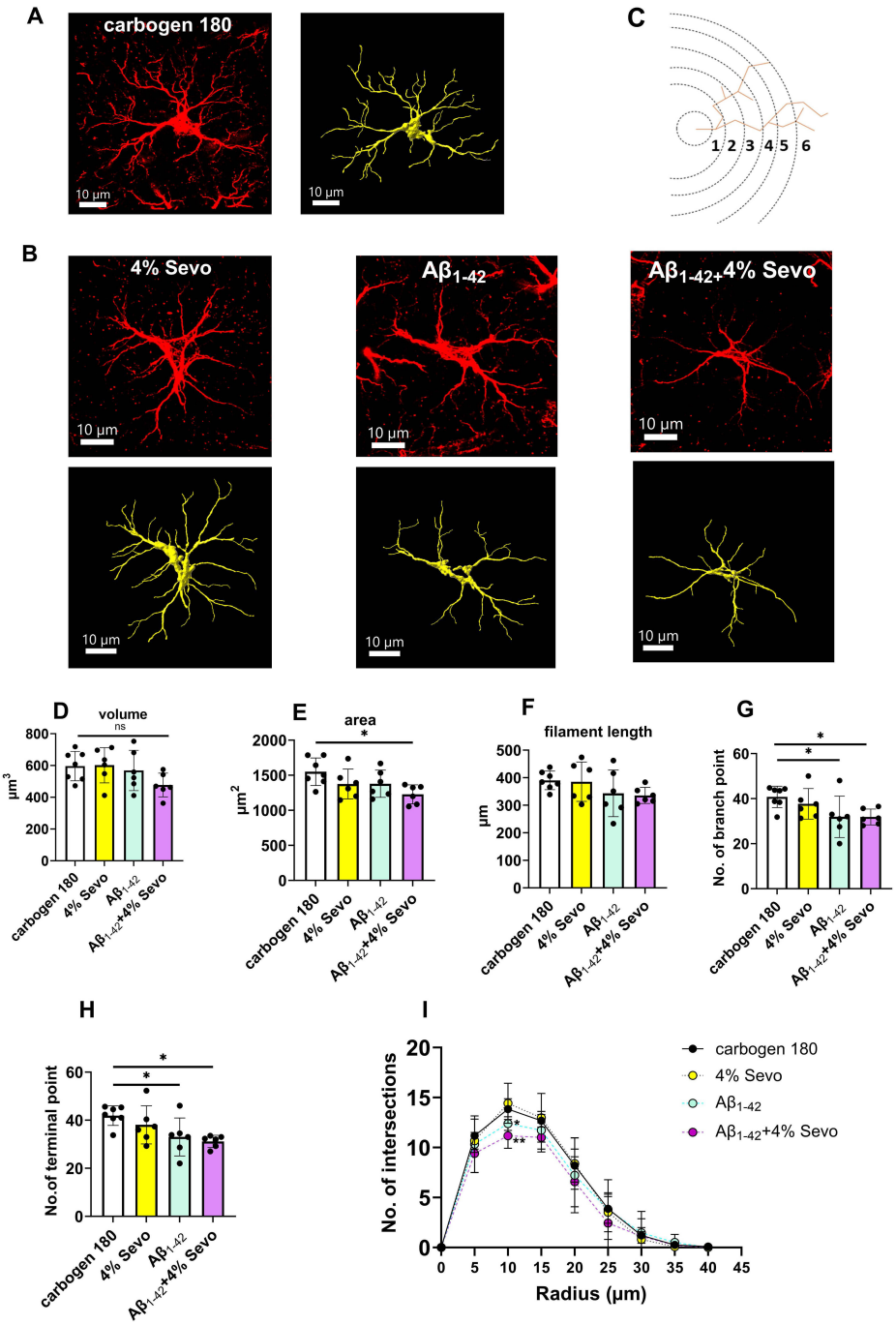

Fig. 2. Sevoflurane and Aβ$_{1-42}$ oligomers together alter the astrocyte morphology. (A) Representative images (left: original, right: reconstructed) of individual astrocytes in hippocampal slices exposed to carbogen (95% O_2/5% CO_2). Scale bar, 10 µm. (B) Representative astrocyte images (original/reconstructed) per treatment group: Sevo, Aβ$_{1-42}$, and Aβ$_{1-42}$ + Sevo. Scale bar, 10 µm. (C) Schematic illustration of Sholl analysis. (D,E) Astrocyte surface area was significantly reduced and the volume showed a trend toward reduction only upon co-exposure to Sevo and Aβ$_{1-42}$. (F) Filament length remained unchanged across all groups. (G,H) Both branch points and terminal points were decreased by Aβ$_{1-42}$ alone, with a further reduction observed under co-exposure. (I) Aβ$_{1-42}$ treatment reduced the number of intersections, an effect significantly exacerbated by sevoflurane co-exposure at a 10 µm radius. Data are presented as mean ± SEM, with individual animals represented by dots (B–I: carbogen 180: n = 7; 4% Sevo, Aβ$_{1-42}$, and Aβ$_{1-42}$+4% Sevo: n = 6, respectively). Statistical significance was determined by one-way ANOVA with Bonferroni's post hoc test for multiple comparisons. ns, not significant; * $p < 0.05$; ** $p < 0.01$.

2.7 Statistical Analysis

Data (presented as mean ± standard error of the mean, SEM) were analyzed via GraphPad Prism 10 (GraphPad Software, San Diego, CA, USA). One-way analysis of variance (ANOVA) with Bonferroni's post-hoc test was employed to compare groups. Statistical significance was defined as $*p < 0.05$. Each data point corresponds to one animal. Each experiment was performed with 6–8 biological replicates, and each biological replicate was measured in triplicate as technical replicates.

3. Results

3.1 Co-Exposure to Sevoflurane and $A\beta_{1\text{-}42}$ Has a Tendency to Increase the 38-KDa GFAP BDP

Given that reliable immobility is necessary during surgical procedures, the clinically recommended target is 1.2 MAC, which can prevent movement in 95% of patients [13]. In C57BL/6 mice, the MAC of sevoflurane is 3.25%; therefore, 1.2 MAC is approximately equivalent to 4% [14].

Studies suggest that GFAP and its BDPs serve as early-stage biomarkers for brain injury and neurodegeneration. Here, we assessed GFAP dynamics in hippocampal slices exposed to 1.2 MAC sevoflurane and/or 50 nM $A\beta_{1\text{-}42}$ using WB (**Supplementary Material**) and immunofluorescence intensity. We observed that sevoflurane and $A\beta_{1\text{-}42}$ together did not affect the expression of intact GFAP; however, there was an increase in the levels of the 38-kDa GFAP breakdown product ($p = 0.08$), with a large effect size (Cohen's d = 1.50). Neither $A\beta_{1\text{-}42}$ nor sevoflurane alone affected BDP levels (Fig. 1A–D). Additionally, co-exposure to sevoflurane and $A\beta_{1\text{-}42}$ significantly reduced GFAP MFI, whereas exposure to either agent alone did not (Fig. 1E,F).

3.2 Co-Exposure to Sevoflurane and $A\beta_{1\text{-}42}$ Synergistically Alters Astrocyte Morphology

The morphology of astrocytes is critically associated with reactive alterations and the progression of AD. In hippocampal slices exposed to $A\beta_{1\text{-}42}$ and/or 1.2 MAC sevoflurane, a synergistic reduction in the structural complexity of astrocytes was observed following co-exposure to $A\beta_{1\text{-}42}$ and sevoflurane (Fig. 2). This finding implies that sevoflurane may potentially influence the pathophysiology of AD.

4. Discussion

AD imposes a significant economic burden and profoundly diminishes patients' quality of life [15]. As the AD population expands, an increasing number of patients require anesthesia for various medical procedures. However, inhalational agents such as sevoflurane may potentially exacerbate the pathophysiology of AD [16]. While the underlying molecular mechanisms remain to be fully elucidated, astrocytes are recognized as core regulators of synaptic homeostasis. Their perisynaptic processes play a pivotal role in maintaining the functional balance of the tripartite synapse [17]. Recent evidence indicates that general anesthetics can induce morphological deficits in astrocytes via the inhibition of Ezrin phosphorylation [18,19]. Our study extends this understanding by demonstrating that this deleterious effect is markedly exacerbated under AD-like conditions. Although morphological alterations in astrocytes have been documented in various AD models—often impacting their functional capacity—the specific interaction between volatile anesthetics and AD pathology remains an area of active investigation. To address this knowledge gap, we examined the effects of the inhalational anesthetic sevoflurane and oligomeric $A\beta_{1\text{-}42}$, both individually and in combination, on astrocytic morphology in acute hippocampal slices.

First, we observed that co-exposure to sevoflurane and $A\beta_{1\text{-}42}$ significantly increased the levels of the 38-kDa GFAP BDP, while leaving intact GFAP and 40–46 kDa GFAP BDPs unaffected. A previous study suggests that elevated levels of GFAP BDPs are indicative of significant astrocytic stress or injury [10]. Consequently, our findings imply that astroglial injury is exacerbated when both sevoflurane and $A\beta_{1\text{-}42}$ are present. Notably, the reduction in GFAP MFI following co-exposure (Fig. 1F) argues against classical reactive astrogliosis, which is typically characterized by cellular hypertrophy and upregulated GFAP expression. Instead, this reduction points toward a phenotype of structural injury or atrophy.

Second, we demonstrated that the co-application of sevoflurane and $A\beta_{1\text{-}42}$ dramatically reduced astrocytic volume, surface area, branching complexity, and Sholl intersections. These features are hallmarks of astrocytic atrophy rather than hypertrophy. This atrophic pattern aligns with literature indicating that astrocytes in the early stages of AD (e.g., in 3× Tg AD mice at 1–3 months of age) undergo atrophy rather than classical activation [20]. Such reductions in morphological complexity and process extension likely impair calcium signaling and disrupt the homeostatic balance of the tripartite synapse.

Moreover, our results demonstrated that co-application of sevoflurane (1.2 MAC) with $A\beta_{1\text{-}42}$ produces a synergistic effect, exacerbating the impact of either sevoflurane (1.2 MAC) or Aβ alone. This could be due to $A\beta_{1\text{-}42}$ primes astrocytes into a vulnerable state (mild calcium dyshomeostasis, oxidative stress, partial calpain activation), and sevoflurane acts as the second hit by further exacerbating calcium dysregulation and inhibiting Ezrin phosphorylation. When combined, the two factors synergistically amplify signaling pathway disruption, pushing the damage beyond the detectable threshold.

Several limitations of this study should be acknowledged. First, to avoid hormonal fluctuations associated with the estrous cycle, we utilized only male mice; thus, our findings may not be generalizable to females. Second, our analysis focused exclusively on hippocampal astrocytes, leaving the response of cortical astrocytes to be determined in

future studies. Furthermore, as this study was conducted in acute hippocampal slices *ex vivo*, the findings may not fully recapitulate the complex systemic environment present *in vivo*.

5. Conclusions

Collectively, our data reveal a synergistic interplay between sevoflurane and oligomeric $A\beta_{1\text{-}42}$, precipitating exacerbated astroglial injury and profound morphological derangements. This synergy, evidenced by elevated GFAP breakdown and compromised structural complexity, suggests that sevoflurane potentiates Aβ-mediated astrocytic dysfunction. These results provide critical mechanistic insights into the exacerbation of AD pathology by general anesthesia, emphasizing the imperative for rigorous perioperative management in susceptible patients.

Availability of Data and Materials

Data are available on reasonable request from the corresponding authors.

Author Contributions

Conceptualization and experimental design, GR, XW and QS; methodology, QS, AKP and SD; writing—original draft preparation, AKP and QS; writing—review and editing, QS, AKP, XW, and GR; supervision, GR and XW. All authors contributed to editorial changes in the manuscript. All authors have read and agreed to the published version of the manuscript. All authors have participated sufficiently in the work and agreed to be accountable for all aspects of the work.

Ethics Approval and Consent to Participate

All animal experiments complied with the Institutional Animal Care and Use Committee regulations of Shanghai University of Traditional Chinese Medicine and ARRIVE guidelines 2.0. The protocol was approved by the Ethics Committee of Shanghai University of Traditional Chinese Medicine (PZSHUTCM2410170001), with experimental arrangements optimized to minimize animal usage and discomfort.

Acknowledgment

Not applicable.

Funding

This project was supported by the Open Fund Program of the Key Laboratory of Anesthesiology and Resuscitation, Union Hospital, Tongji Medical College, Huazhong University of Science and Technology, China (2024MZFS003).

Conflicts of Interest

The authors declare no conflicts of interest.

Supplementary Material

Supplementary material associated with this article can be found, in the online version, at https://doi.org/10.31083/JIN50442.

References

[1] Rajmohan R, Reddy PH. Amyloid-Beta and Phosphorylated Tau Accumulations Cause Abnormalities at Synapses of Alzheimer's disease Neurons. Journal of Alzheimer's Disease: JAD. 2017; 57: 975–999. https://doi.org/10.3233/JAD-160612

[2] Lei M, Xu H, Li Z, Wang Z, O'Malley TT, Zhang D, et al. Soluble Aβ oligomers impair hippocampal LTP by disrupting glutamatergic/GABAergic balance. Neurobiology of Disease. 2016; 85: 111–121. https://doi.org/10.1016/j.nbd.2015.10.019

[3] Dong Y, Zhang G, Zhang B, Moir RD, Xia W, Marcantonio ER, et al. The common inhalational anesthetic sevoflurane induces apoptosis and increases beta-amyloid protein levels. Archives of Neurology. 2009; 66: 620–631. https://doi.org/10.1001/archneurol.2009.48

[4] Ramos Ramos V, Mesa Suárez P, Santotoribio JD, González García MÁ, Muñoz Hoyos A. Neuroprotective effect of sevoflurane in general anaesthesia. Medicina Clinica. 2017; 148: 158–160. https://doi.org/10.1016/j.medcli.2016.10.039

[5] Shi Q, Wang X, Pradhan AK, Fenzl T, Rammes G. The Effects of Sevoflurane and Aβ Interaction on CA1 Dendritic Spine Dynamics and MEGF10-Related Astrocytic Synapse Engulfment. International Journal of Molecular Sciences. 2024; 25: 7393. https://doi.org/10.3390/ijms25137393

[6] Verkhratsky A, Rodrigues JJ, Pivoriunas A, Zorec R, Semyanov A. Astroglial atrophy in Alzheimer's disease. Pflugers Archiv: European Journal of Physiology. 2019; 471: 1247–1261. https://doi.org/10.1007/s00424-019-02310-2

[7] Tykhomyrov AA, Pavlova AS, Nedzvetsky VS. Glial Fibrillary Acidic Protein (GFAP): on the 45th Anniversary of Its Discovery. Neurophysiology. 2016; 48: 54–71. https://doi.org/10.1007/s11062-016-9568-8

[8] Porchet R, Probst A, Bouras C, Dráberová E, Dráber P, Riederer BM. Analysis of glial acidic fibrillary protein in the human entorhinal cortex during aging and in Alzheimer's disease. Proteomics. 2003; 3: 1476–1485. https://doi.org/10.1002/pmic.200300456

[9] Korolainen MA, Auriola S, Nyman TA, Alafuzoff I, Pirttilä T. Proteomic analysis of glial fibrillary acidic protein in Alzheimer's disease and aging brain. Neurobiology of Disease. 2005; 20: 858–870. https://doi.org/10.1016/j.nbd.2005.05.021

[10] Yang Z, Arja RD, Zhu T, Sarkis GA, Patterson RL, Romo P, et al. Characterization of Calpain and Caspase-6-Generated Glial Fibrillary Acidic Protein Breakdown Products Following Traumatic Brain Injury and Astroglial Cell Injury. International Journal of Molecular Sciences. 2022; 23: 8960. https://doi.org/10.3390/ijms23168960

[11] Pradhan AK, Shi Q, Tartler KJ, Rammes G. Quantification of astrocytic synaptic pruning in mouse hippocampal slices in response to ex vivo Aβ treatment via colocalization analysis with C1q. STAR Protocols. 2022; 3: 101687. https://doi.org/10.1016/j.xpro.2022.101687

[12] Althammer F, Krause EG, de Kloet AD, Smith J, Grinevich V, Charlet A, et al. Identification and three-dimensional reconstruction of oxytocin receptor expressing astrocytes in the rat and mouse brain. STAR Protocols. 2022; 3: 101160. https://doi.org/10.1016/j.xpro.2022.101160

[13] de Jong RH, Eger EI, 2nd. MAC expanded: AD50 and AD95 values of common inhalation anesthetics in man. Anesthesiology. 1975; 42: 384–389.

[14] Cesarovic N, Nicholls F, Rettich A, Kronen P, Hässig M, Jirkof P, et al. Isoflurane and sevoflurane provide equally effective anaesthesia in laboratory mice. Laboratory Animals. 2010; 44: 329–336. https://doi.org/10.1258/la.2010.009085

[15] Wimo A, Guerchet M, Ali GC, Wu YT, Prina AM, Winblad B, et al. The worldwide costs of dementia 2015 and comparisons with 2010. Alzheimer's & Dementia: the Journal of the Alzheimer's Association. 2017; 13: 1–7. https://doi.org/10.1016/j.jalz.2016.07.150

[16] Arora SS, Gooch JL, García PS. Postoperative cognitive dysfunction, Alzheimer's disease, and anesthesia. The International Journal of Neuroscience. 2014; 124: 236–242. https://doi.org/10.3109/00207454.2013.833919

[17] Ghézali G, Dallérac G, Rouach N. Perisynaptic astroglial processes: dynamic processors of neuronal information. Brain Structure & Function. 2016; 221: 2427–2442. https://doi.org/10.1007/s00429-015-1070-3

[18] Chen L, Jiao J, Lei F, Zhou B, Li H, Liao P, et al. Ezrin-mediated astrocyte-synapse signaling regulates cognitive function via astrocyte morphological changes in fine processes in male mice. Brain, Behavior, and Immunity. 2025; 124: 177–191. https://doi.org/10.1016/j.bbi.2024.11.022

[19] Zhou B, Li Q, Su M, Liao P, Luo Y, Luo R, et al. Astrocyte morphological remodeling regulates consciousness state transitions induced by inhaled general anesthesia. Molecular Psychiatry. 2025; 30: 4006–4022. https://doi.org/10.1038/s41380-025-02978-2

[20] Yeh CY, Vadhwana B, Verkhratsky A, Rodríguez JJ. Early astrocytic atrophy in the entorhinal cortex of a triple transgenic animal model of Alzheimer's disease. ASN Neuro. 2011; 3: 271–279. https://doi.org/10.1042/AN20110025